Eur. Phys. J. B **59**, 503–508 (2007)
DOI: 10.1140/epjb/e2007-00311-4

THE EUROPEAN PHYSICAL JOURNAL B

Thermal and thermoelectric behavior of silicon-germanium quantum well structures

M.N. Tripathi[1,2,a] and C.M. Bhandari[1,3]

[1] Department of Physics, University of Allahabad, Allahabad 211002, India
[2] C.M.P. College, Allahabad 211002, India
[3] Indian Institute of Information Technology, Allahabad 211002, India

Received 26 June 2007
Published online 15 November 2007 –

Abstract. Tailoring thermoelectric materials for specific designs and applications has been gaining momentum during past three decades. Initially confined to conventional (bulk) framework an entirely new scenario emerged with inclusion of low-dimensional structures in the scheme of things. The paper examines the effect of size reduction on phonon and electron properties in two-dimensional (quantum well) structures with an aim to maximize thermoelectric performance. The formulation has been applied to silicon-germanium quantum wells with well width ranging from 50–500 Å aimed at finding best alloy combination for thermoelectric applications.

PACS. 73.50.Lw Thermoelectric effects – 73.63.Hs Quantum wells – 73.61.Ey III-V semiconductors

1 Introduction

Search for advanced thermoelectric materials with improved figure-of-merit has been closely linked with an increased understanding of electronic and phonon properties in semiconductors. During the early part of the second half of twentieth century considerable research activity in seeking reduction in phonon thermal transport resulted in the study of highly disordered systems [1–3]. The effect of disorder scattering was to substantially scatter high frequency phonons, the remaining low frequency phonons could then be effectively scattered at grain boundaries. This led to in-depth study of fine-grained disordered semiconductor alloys such as PbTe-SnTe, PbTe-PbSe and Si-Ge to name only a few. These studies [4–6] veered around bulk electron and phonon properties with efforts to maximize the scattering of phonons without adversely affecting the electrical to thermal conductivity ratio σ/λ. Thermoelectric behavior of bulk material is expressed in terms of transport coefficients such as electrical conductivity, Seebeck coefficient and thermal conductivity [7–9].

The next logical step in the search for advanced materials was to go beyond the usual bulk framework. In the fine-grained structures or thin films phonon (electron) density-of-states and dispersion relations hold good and the only effect of grain size appears in phonon (electron) mean-free-path due to increased boundary scattering. A further size reduction brings into focus quantum effects which may include energy distribution and energy-wave vector relations. Last two decades have witnessed an intense research activity in low-dimensional structures that could provide improved thermoelectric materials [10–17].

Model calculations for free-standing as well as embedded well structures [18–24] take into consideration modifications of the transport equations in the continuum approximation and with proper boundary conditions. Phonon modes in wells have been calculated by Bannov et al. [25] and Svizhenko et al. [26]. By solving the elasticity equation

$$\frac{\partial^2 \vec{u}}{\partial t^2} = v_l^2 \nabla^2 \vec{u} + \left(v_l^2 - v_t^2\right) \mathrm{grad}\,\mathrm{div}\,\vec{u} \qquad (1)$$

where $\vec{u}$ is the displacement vector, and v_l and v_t are the speeds of longitudinal and transverse elastic waves (in the bulk), respectively. It is important to take account of the boundary conditions in free-standing wells where normal component of the stress tensor vanishes. This brings about a significant change in phonon dispersion relations. The boundary condition will change for the embedded structure with the normal component of the stress tensor being nonzero whereas the displacement vanishes at the boundary.

In this paper we present an analysis of the effect of spatial confinement of acoustic phonons on thermal transport coefficients and thermoelectric figure-of-merit of free-standing quantum well structures for different alloy compositions of $Si_XGe_{(1-X)}$ (X ranging from 0.3 upto 0.8) aimed at finding the best alloy composition for thermoelectric applications.

[a] e-mail: ommadhav27@rediffmail.com

2 Theory

2.1 Thermal transport

Study of thermal transport in semiconductors requires the contributions from phonons as well as electron (hole). In bulk, phonon contribution is largely influenced by phonon-phonon scattering and disorder scattering. However, in quantum wells a significant drop in phonon group velocity is observed due to their spatial confinement. The change in phonon dispersion may lead to a decrease in-group velocity, resulting in a corresponding increase in relaxation rates. This may have a significant effect on the in-plane lattice thermal conductivity [27]. The lattice thermal conductivity at a temperature T is given as

$$\lambda_L = \frac{1}{2\,\pi^2} \int v_G^2\ (\cos\phi)^2\ \tau_C\,(q)\ C_{ph}\,(q)\ d^3q \qquad (2)$$

where v_G is the phonon group velocity, ϕ is the angle between the group velocity and direction of heat flow, q is phonon wave vector, $\tau_C\,(q)$ is combined phonon relaxation time, $C_{ph}\,(q)$ is specific heat. For in-plane transport along x-axis, $\cos\phi = 1$. Within the framework of Debye approximation, the effect of acoustic phonon confinement could lead to decreased phonon group velocity, increased phonon relaxation rate and modified phonon density of states (PDOS). Disregarding the PDOS modification, the expression for lattice thermal conductivity transforms as [27]

$$\lambda_L = \frac{k_B}{(2\pi^2)} \left(\frac{k_B}{\hbar}\right)^3 T^3 \int_0^{\theta/T} \frac{\tau_C\,(x)\ x^4\,e^x}{v_G\,(x)\ (e^x-1)^2} dx \qquad (3)$$

where $x = \frac{h\upsilon}{k_B\,T}$, k_B is Boltzmann constant, θ is Debye temperature.

Considering the fact that only those processes that do not conserve crystal momentum contribute to the lattice thermal conductivity, $\tau_C\,(x)$ takes into account processes such as boundary scattering (τ_B), mass-difference scattering (τ_I) and three phonon Umklapp scattering (τ_U) [18]. The total relaxation rate is defined as

$$\frac{1}{\tau_C} = \frac{1}{\tau_U} + \frac{1}{\tau_I} + \frac{1}{\tau_B}. \qquad (4)$$

The phonon dispersion in quantum well structures is used in calculating the relaxation rates which is quite different from the bulk. Mass-difference scattering is strongly affected by the change in average phonon group velocity. In the present paper we propose to investigate the Si-Ge quantum well structures, hence this scattering mechanism is of main interest and is given by [28,29]

$$\frac{1}{\tau_I} = \frac{V_0\,\omega^4}{4\pi\,v_G^3} \sum_i f_i\,[1-(M_i/M)]^2 \qquad (5)$$

where V_0 is the volume per atom, M_i is the mass of an atom, and f_i is the fractional content of atoms with mass M_i and M is mean atomic mass. Phonon-phonon scattering relaxation time is assumed to be same as in bulk except for the modification in group velocity due to confinement effects. Balandine et al. [18] have reported a small contribution of umklapp processes with major scattering caused by impurity. The relaxation time for boundary scattering considering semi empirical relation is given by [30]

$$\frac{1}{\tau_B} = \frac{v_G}{a} \qquad (6)$$

where a is the width of quantum well.

2.2 Phonon confinement

Phonon scattering rates strongly depend on group velocity and influence thermal transport. Free-standing structures may be as small as a few interatomic distances, and also the electrons (holes) energy in these structures is quantized. Phonon system is also quantized and quantization of the acoustic phonon spectrum in a similar manner to that of electron quantization should occur. Three types of confined acoustic modes in quantum well structures are characterized by their distinctive symmetries [31]; Shear waves (S), Dilatational waves (D) and Flexural waves (F). The shear mode has only one nonzero component of displacement vector in the perpendicular direction of wave propagation. The dilatational and flexural phonon modes have two non-zero components in which one component lies in the direction of propagation. It is possible to show analytically the dependence of the in-plane phonon group velocity on the cross-plane phonon quantisation for shear modes.

For evaluating in-plane thermal conductivity only shear waves are considered. Quantisation effects will be significant for transverse waves with atomic displacement along z-direction. For cross-plane thermal transport dilatational and flexural modes will show quantization effect. The phonon dispersion relation for shear modes is written as [31]

$$\omega_n = v_T \sqrt{\left(q_{Z,n}^2 + q_X^2\right)} \qquad (7)$$

here $q = q_X$ is the phonon wave vector along in-plane direction and n denotes the different branches of the same polarization type, v_T is the transverse phonon velocity in the bulk. The phonon wave vector along the confinement direction ($q_{Z,n}$) is quantized. The dispersion relation can now be written as

$$\omega_n = v_T \sqrt{\left(\left(\frac{\pi\,n}{a}\right)^2 + q^2\right)}. \qquad (8)$$

The phonon group velocity for each mode type in the nth branch is defined as $v_{G,n} = \frac{\partial\omega_n}{\partial q}$, and is expressed as

$$v_{G,n}\,(q) = \frac{v_T}{\sqrt{\left(\frac{\pi\,n}{q\,a}\right)^2 + 1}}. \qquad (9)$$

Expressing group velocity in terms of phonon energy

$$v_{G,n}(\hbar\omega) = v_T\sqrt{1-\left(\frac{\hbar\, v_T\,\pi\, n}{\hbar\,\omega_n\, a}\right)^2}. \tag{10}$$

In order to obtain resulting average group velocity, all modes are considered for a given energy

$$\bar{v}_G(\hbar\,\omega) = \frac{\sum\limits_n v_{G,n}(\hbar\,\omega)\; N_n(\omega)}{\sum\limits_n N_n(\omega)} \tag{11}$$

where $v_{G,n}$ is the group velocity of nth mode and $N_n(\omega)$ is number of oscillators with frequency ω on the nth mode and is given as $N_n(\omega) \;\propto\; \exp\left(-\frac{n\,\hbar\,\omega}{k_B\,T}\right)$.

After obtaining average phonon group velocity for all mode contributions at a given temperature and width (of quantum well), the relaxation rate is obtained by equation (4) which is now different from the bulk relaxation rate as it consists the confinement effect of acoustic phonons in quantum well structures. The lattice thermal conductivity for quantum wells can be obtained with the help of equation (3).

2.3 Electronic properties

In quantum well structures, electron density of states is significantly different from usual parabolic variation in the bulk. The size quantum limit (SQL) assumption [32] that electrons occupy only the lowest sub-band is incorporated into theoretical calculations to obtain size related effects on transport coefficients. A quantum well is related to electron confinement only in one direction (say z-direction) and the particle is free to move in other directions. The electron wave function and energy eigenvalues are given [33]

$$\psi = \left(\frac{2}{\Omega}\right)^{1/2}\exp(ik_x x + ik_y y)\sin\left(\frac{n\pi z}{a}\right) \tag{12}$$

$$E = E_n + \frac{\hbar^2 k_{II}^2}{2m} \tag{13}$$

where $E_n = \frac{\pi^2\hbar^2}{2m_z a^2}n^2$, $k_{II}^2 = k_x^2 + k_y^2$.

m_z is effective mass of electron along confinement axis and m is effective mass of electron along free axis. Ω is total volume of the sample and 'a' is well width. 'n' is a quantum number. For two-dimensional structures acoustic phonon scattering relaxation rate can be written as [34]

$$\frac{1}{\tau_{ac}} = \frac{3\mathrm{E}_D^2 m}{\rho\,\hbar^2 a} \tag{14}$$

where, E_D is deformation potential, ρ is density of material. The electrical conductivity, Seebeck coefficient and Lorenz factor can be written as [33]

$$\sigma = \frac{1}{2\pi\, a}\left(\frac{2k_B T}{\hbar^2}\right)\sqrt{\frac{m_y^*}{m_x^*}}e^2\tau_0 I_6 \tag{15}$$

$$\alpha = \frac{k_B}{e}\left[\frac{E_F}{k_B T} - \frac{I_4 + I_5}{I_6}\right] \tag{16}$$

$$L_f = \left[\frac{I_1 + 2I_2 + I_3}{I_6} - \left(\frac{I_4 + I_5}{I_6}\right)^2\right] \tag{17}$$

where integrals I_1, I_2, I_3, I_4, I_5 and I_6 are defined as

$$I_1 = \sum_{n=1}^{E_n \leqslant E_F}\int_0^\infty x^2 D(x)\; dx,$$

$$I_2 = \sum_{n=1}^{E_n \leqslant E_F} E_n^{'}\int_0^\infty x D(x)\; dx,$$

$$I_3 = \sum_{n=1}^{E_n \leqslant E_F}\left(E_n^{'}\right)^2\int_0^\infty D(x)\; dx,$$

$$I_4 = \sum_{n=1}^{E_n \leqslant E_F}\int_0^\infty x D(x)\; dx,$$

$$I_5 = \sum_{n=1}^{E_n \leqslant E_F} E_n^{'}\int_0^\infty D(x)\; dx,$$

$$I_6 = \sum_{n=1}^{E_n \leqslant E_F}\int_0^\infty D(x)\; dx,$$

where $D(x) = x\left(-\frac{\partial f_n}{\partial x}\right)$, Fermi distribution function $f_n = \frac{1}{e^{x-\eta_n}+1}$, $E_n^{'} = \frac{E_n}{k_B T}$ and $\eta_n = \frac{E_F}{k_B T} - \frac{E_n}{k_B T}$. We have taken the contribution of only lowest sub-band in the framework of SQL.

2.4 Results and discussion

$\mathrm{Si}_X\mathrm{Ge}_{(1-X)}$ alloys are amongst the most thoroughly investigated alloy systems for their usefulness in thermoelectric high temperature applications. However, most of these studies are confined to bulk properties. In the present study we have examined the usefulness of the alloy system in the form of quantum well structures. The study centers primarily on $\mathrm{Si}_X\mathrm{Ge}_{(1-X)}$ alloys for X ranging from 0.3 upto 0.8 to obtain the best alloy composition for thermoelectric purposes. Physical parameters for Si and Ge at room temperature are presented in Table 1. Relevant parameters for various alloy compositions have been obtained by linear interpolation. However, effective electron masses for alloy combinations with $x \geqslant 0.15$ are same as that of silicon [35].

We shall be primarily interested in the in-plane transport. Calculations of phonon group velocity as function of in-plane wave vector for shear modes have been performed

Table 1. Physical parameters for Si and Ge at room temperature

	Density(ρ) (Kg/m^3)	Transverse Phonon velocity (v_T) (m/s)	Lattice Parameter (A°)	Elastic Constant (C11) (10^{11}Nm^{-2})	Deformation Potential (E_D) (eV)	$\frac{m_l}{m_0}$	$\frac{m_t}{m_0}$
Si	2330	5845	5.43	1.66	12.8	0.98	0.19
Ge	5323	3542	5.658	1.28	12.9	1.6	0.08

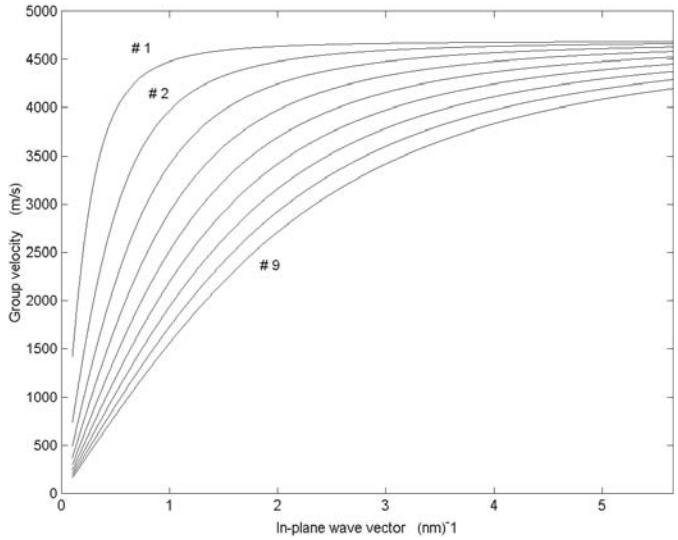

Fig. 1. Variation of the phonon group velocity plotted against in-plane wave vector for shear modes in a 100 Å wide quantum well for the alloy composition $Si_{0.5}Ge_{0.5}$. The nine lowest phonon modes are shown.

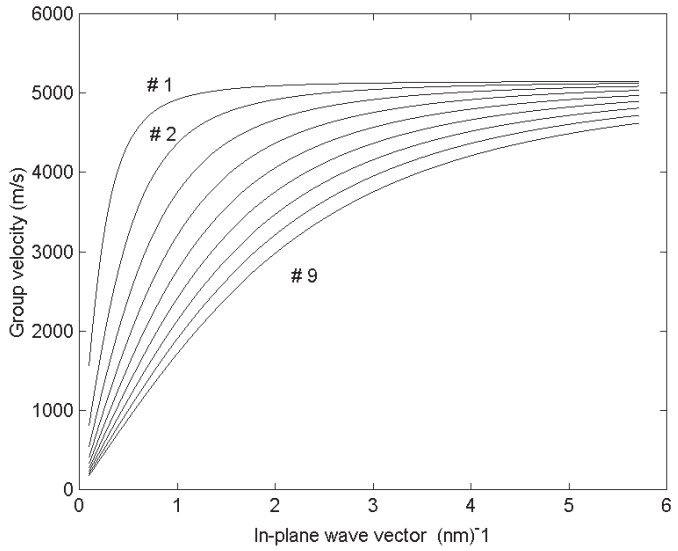

Fig. 2. Phonon group velocity for nine lowest phonon modes plotted against in-plane wave vector for shear modes in a 100 Å wide quantum well for alloy composition $Si_{0.7}Ge_{0.3}$.

for various alloy combinations and well widths. However, here we present the results only for two alloy combinations ($X = 0.5, 0.7$) for 100 Å well width in Figures 1 and 2. The dispersion between various branches is significant in the region of 'q' ranging from 0.5 to 4 nm^{-1}.

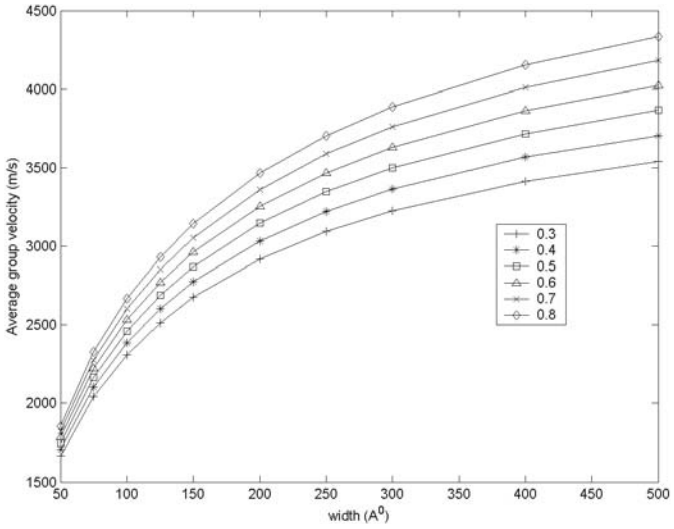

Fig. 3. Plot of average group velocity against well width for different alloy compositions of $Si_XGe_{(1-X)}$ with X ranging from 0.3 to 0.8.

Figure 3 shows variation of average group velocity against well width for different alloy compositions taking into consideration the contributions of all phonon modes in each alloy. It is obvious that the value of average group velocity is lower for lower silicon content. The value of average group velocity for each alloy composition becomes almost half the bulk value for 100 Å well width. Moreover, average group velocity $\bar{v}_G$ falls rapidly below 100 Å. For the lower values of well width the dispersion in the curves is small and around 50 Å and below $\bar{v}_G$ decreases sharply and is relatively independent of variation in alloy composition.

Figure 4 displays the variation of room temperature lattice thermal conductivity for different alloy compositions of $Si_XGe_{(1-X)}$ against well width. One can notice immediately that the alloy combination which gives minimum lattice thermal conductivity is not very different from that of the bulk. In the bulk $X \sim 0.7$ composition has the lowest value of lattice thermal conductivity. Phonon scattering rate is mainly affected by alloy disorder with major changes resulting from the effect of confinement on phonon group velocity. The strong effect of spatial confinement of acoustic phonons on lattice thermal conductivity λ_L is clearly evident from the results.

Figure 5 shows variation of electrical conductivity against well width 'a' of free-standing quantum wells of $Si_XGe_{(1-X)}$at $T = 300$ K. The value of electrical conductivity is almost constant for higher value of 'a' in each alloy composition and decreases rapidly below 100 Å.

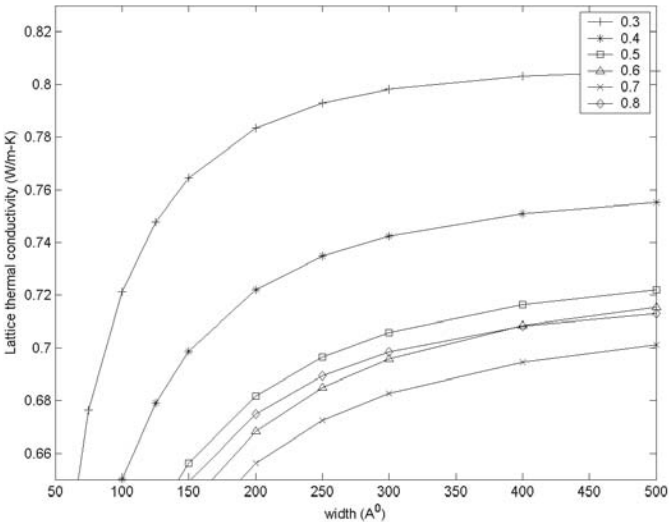

Fig. 4. Variation of lattice thermal conductivity versus well width at room temperature for different alloy compositions of $Si_X Ge_{(1-X)}$.

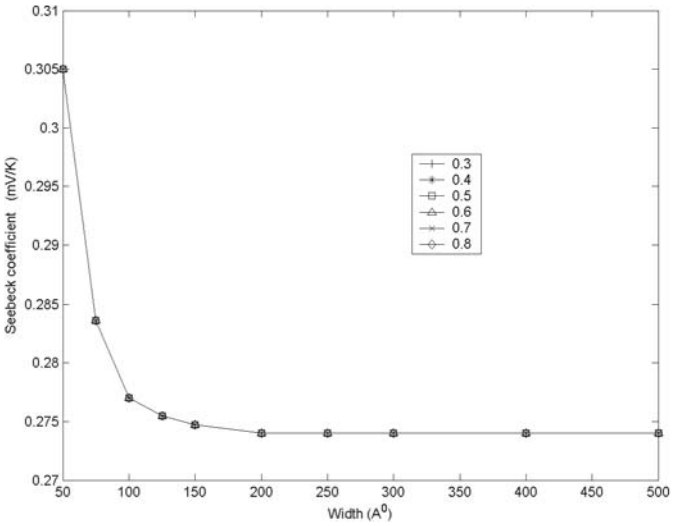

Fig. 6. Variation of Seebeck coefficient with well width for various alloy combinations.

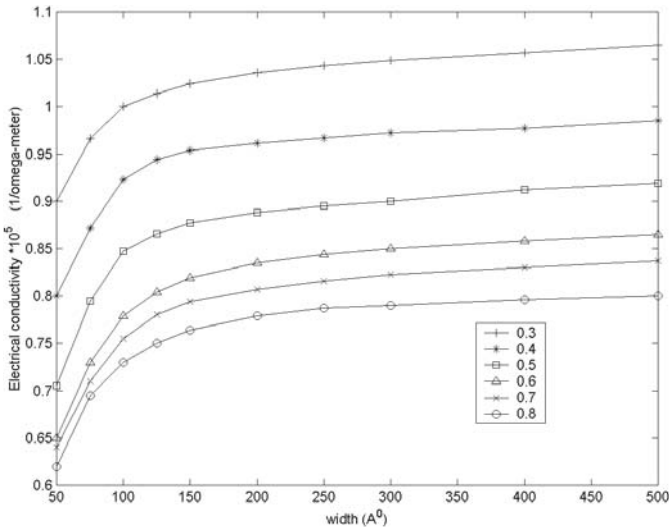

Fig. 5. Plot of electrical conductivity against well width at $T = 300$ K.

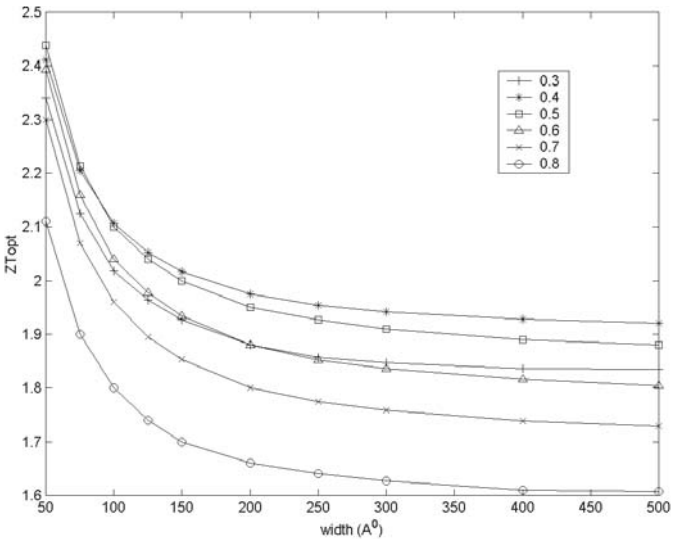

Fig. 7. Optimized dimensionless figure-of-merit plotted against well width at room.

Figure 6 provides the variation of Seebeck coefficient with well width and alloy compositions at room temperature. The Seebeck coefficient is independent of alloy composition and increases sharply below 100 Å.

Figure 7 gives the variation of optimized dimensionless figure-of-merit against well width. For almost all alloy compositions the value of ZT_{opt} approaches 2 or more. For quantum wells the alloy composition for best thermoelectric performance corresponds to $X \sim 0.4$–0.5 unlike the bulk case where the best composition corresponds to $X \sim 0.7$ [36]. The sharp rise in ZT_{opt} below 100 Å is of significance in thermoelectric applications. This sharp rise is primarily due to changes both in Seebeck coefficient as well as the electrical to thermal conductivity ratio which tend to favour high values of thermoelectric figure-of-merit. It is due to significant contributions from electronic properties that the best alloy combination is no more determined solely by changes in lattice thermal transport as in bulk.

The authors are thankful to Dr. M.D. Tiwari, Prof. Hari Prakash for their interest and support. M.N. Tripathi thankfully acknowledges Dr. Suneet Dwivedi and Dr. M.P. Singh for helpful discussions and technical support.

References

1. H.J. Goldsmid, A.W. Penn, Phys. Lett. **27A**, 523 (1968)
2. J.E. Parrott, J. Phys. C: Sol. State Phys. **2**, 147 (1969)
3. C.M. Bhandari, D.M. Rowe, J. Phys. D: Appl. Phys. **10**, L59 (1977)

4. H.R. Meddins, J.E. Parrott, J. Phys. C: Sol. State Phys. **9**, 1263 (1976)
5. C.M. Bhandari, D.M. Rowe, J. Phys. C: Sol. State Phys. **11,** 1787 (1978)
6. C.M. Bhandari, D.M. Rowe, Contemp. Phys. **21**, 219 (1980)
7. D.M. Rowe, C.M. Bhandari, *Modern Thermoelectrics* (Reston Publishing Company, Virginia, 1983)
8. C.M. Bhandari, D.M. Rowe, *Thermal Conduction in Semiconductors* (Wiley Eastern Limited, New Delhi, 1988), Chaps. 3 and 4.
9. G.D. Mahan, *Sol. State Physics*, Good Thermoelectrics, edited by H. Ehrenreich, F. Saepen (Academic Press, San Diego, 1998), Vol. 51
10. L.D. Hicks, M.S. Dresselhaus, Phys. Rev. B **47**, 12727 (1993)
11. J.O. Sofo, G.D. Mahan, Appl. Phys. Lett. **65**, 2690 (1994)
12. D.A. Broido, T.L. Reinecke, Phys. Rev. B **51**, 13797 (1995)
13. L.D. Hicks, M.S. Dresselhaus, Phys. Rev. B **47**, 16631 (1993)
14. C.M. Bhandari, in *Thermoelectrics Handbook: Macro to Nano*, edited by D.M. Rowe (CRC Press, FL, 2006)
15. M.S. Dresselhaus, 6.732 *Solid State Physics*, Part 1: *Transport properties of solids*, Lecture Notes, Chap. 9, p. 139 (Fall, 2001)
16. T. Koga, X. Sun, S.B. Cronin, M.S. Dresselhaus, K.L. Wang, G. Chen, J. Comput. Aided Mater. Des. **4**, 175 (1997)
17. A. Balandin, Phys. Low - Dim. Struct. 1/2, 1 (2000)
18. A. Balandin, K.L. Wang, Phys. Rev. B **58**, 1544 (1998)
19. A. Balandin, K.L. Wang, J. Appl. Phys. **84**, 6149 (1998)
20. T.C. Harman et al., in *Proceedings of 18th International Conference on Thermoelectrics*, edited by A. Ehrlich (Piscataway, NJ, 1999), pp. 280–284
21. R. Venkatasubramanian et al., Nature **413**, 597 (2001)
22. S.M. Lee, D.G. Cahill, R. Venkatasubramanian, Appl. Phys. Lett. **70**, 2957 (1997)
23. E.I. Rogacheva, O.N. Nashchekina, S.N. Grigorov, M.A. Us, M.S. Dresselhaus, S.B. Cronin, Nanotechnology **14**, 53 (2003)
24. E.I. Rogacheva, O.N. Nashchekina, S.N. Grigorov, K.A. Nasedkin, M.S. Dresselhaus, S.B. Cronin, Appl. Phys. Lett. **80**, 2690 (2002)
25. N. Bannove, V. Mitin, M. Strocio, Phys. Stat. Sol. B **183**, 131 (1994)
26. A. Svizhenko, A. Balandin, S. Bandopadhyaya, M.A. Stroscio, Phys. Rev. B **57**, 4687 (1998)
27. A. Balandin, Phys. Low - Dim. Struct. **5/6**, 73 (2000)
28. P.G. Klemens, in *Sol. State Physics*, edited by F. Seitz, D. Turnbull (Academic, New York, 1958), Vol. 7, p. 1
29. J.E. Parrot, A.D. Stuckes, *Thermal Conductivity of Solids* (Methuen, New York, 1975)
30. J. Callaway, Phys. Rev. **113**, 1046 (1959)
31. N. Bannove, V. Aristove, V. Mitin, Phys. Rev. B **51**, 9930 (1995)
32. S.S. Kubakaddi, B.G. Mulimani, J. Appl. Phys. **58**, 3643 (1985)
33. M.P. Singh, C.M. Bhandari, Sol. State Communications **133**, 29 (2005)
34. B.K. Ridley, *Electrons and Phonons in Semiconductors Multilayers* (Cambridge University Press, USA, 1997), Chaps. 2 and 11
35. F. Schaffler, *Properties of Advanced Semiconductor materials*, edited by M.E. Levinshtein, S.L. Rumyantsev, M.S. Shur (John Wiley & Sons, New York, 2001), pp. 149–188
36. M.N. Tripathi, C.M. Bhandari, J. Phys.: Condens. Matter **15**, 5359 (2003)